Post Stall Propeller Behavior
at Low Reynolds Numbers

Daniel V. Uhlig,[*] and Michael S. Selig[†]

Department of Aerospace Engineering, University of Illinois at Urbana–Champaign

Limited data exists for propeller and wind turbine post stall aerodynamics. Post stall aerodynamics was observed in small propellers at low Reynolds numbers. First, performance data (thrust, power, and efficiency) for a set variable pitch propellers was acquired in a wind tunnel. The propellers were 6 to 9.9 inches in diameter and were able to pitch to extreme angles. Second detailed geometric characteristics (pitch, chord, airfoil) of the propellers were measured. Finally, PROPID with and without stall delay models was used to simulate the propellers and predict the performance. Comparing the experimental and calculated results identified regions where post stall aerodynamics affected propeller performance.

I.   Introduction

SMALL scale propeller performance is difficult to predict because of the low Reynolds numbers and post stall aerodynamics. Experimental data helps improve the modeling of small scale propellers and allows better propellers to be designed.

Blade Element Momentum Theory (BEMT) can be used to quickly predict propeller performance. The basis of BEMT is commonly available 2-D airfoil performance data from either experimental or computational results. It also allows each section of the propeller or wind turbine to be designed and optimized using a computer code such as PROPID.[1] However, BEMT method has limited accuracy when the 2-D airfoil is at angles of attack beyond stall. Particularly at lower advance ratios the performance is under predicted by BEMT because of the post stall behavior of the blades. Instead of the assumed 2-D airfoil flow, the flow actually is much more complicated with significant radial components. Wind turbine investigations by Tangler and Kocurek[2] have shown significant post-stall lift. Using an instrumented 33-ft diameter rotor with numerous pressure taps along the blades, local C_l was found. From the pressure taps and computational data they postulated that a second standing vortex developed behind the rotor blade. This vortex acted as an endplate, increasing the lift generated by the inboard sections.

Himmelskamp discovered the effect of propeller airfoil sections performing better than 2-D predictions in 1945.[3] A number of studies and techniques have been developed to cope with the post-stall effects. Most of the techniques were developed and are used within the wind turbine industry. Within PROPID, Selig[4] implemented a number of post-stall models to estimate post-stall aerodynamics. These estimates have been useful to better model horizontal axis wind turbines.

For propellers, Gur and Rosen[5] took existing test data from 5.33-ft diameter pitchable propeller and applied BEMT to predict the performance. The basic predictions with 2-D airfoil data had good accuracy at higher advance ratios, but it under predicted performance at lower advance ratios. By applying post-stall corrections the correlation between the predicted and actual test data at low advance ratios improved.

The propellers tested had diameters of 6 to 9.9 in. For the most part these small diameter propellers operated at chord Reynolds numbers less than 100,000. Inboard sections had values below 20,000. At these values, airfoil performance, particularly drag, is significantly dependent on the Reynolds number.

---

[*]Graduate Student, Department of Aerospace Engineering UIUC, duhlig2@uiuc.edu, and AIAA Student Member.

[†]Associate Professor, Department of Aerospace Engineering, m-selig@uiuc.edu, and AIAA Senior Member.

American Institute of Aeronautics and Astronautics

In this experiment, many similar shaped pitchable propellers were used to investigate the post-stall effects. The propellers had 6 to 9.9 in. diameters, two types of tapering, and settable pitch. The propellers blades are shown in Fig. 1. The propeller pitch was set to a low, medium and high setting. Each time the pitch at 75% radius was recorded. Performance data was also recorded over a range of advance ratios at a few RPM settings by sweeping the wind tunnel speed.

The propeller geometries were measured by cutting each blade at approximately every quarter inch along the blade radius. The geometric data was used to generated predicted performance using PROPID. Cross sections were used to generate 2-D airfoil performance data and then predict the propeller performance. The geometric-based predictions were compared with the experimental data to show where post-stall airfoil aerodynamics significantly affects propeller performance.

Figure 1. The variable pitch propeller blades.

II.   Experimental Setup

This section outlines the capabilities of the UIUC wind tunnel and propeller test instrumentation. The experimental setup was originally developed by Brandt[6] and Tehrani.[7] To test the selected propellers, the test apparatus needed no modifications. The low speed wind tunnel facility at UIUC is seen in Fig. 2 and has a small propeller test apparatus for use in the open return wind tunnel. The test section is 2.8 ft (height) by 4.0 ft (width) by 8 ft (length). A 125-hp AC motor powers the tunnel with flow speeds up to 235 ft/sec. For the propeller testing, the maximum speed was limited to 80 ft/sec.[7,9] A honeycomb layer 4-inches thick at the inlet along with four additional screens minimizes turbulence to increase the flow quality. The measured turbulence in the UIUC wind tunnel was found to be less then 0.1% by Selig.[8]

To obtain the experimental propeller performance characteristics (C_T vs J and C_P vs. J) the following quantities were measured experimentally in the wind tunnel:

- freestream velocity (ft/sec)
- propeller rotation speed (RPM)
- torque (oz/in)
- thrust (oz)

Thrust and torque were measured using the experimental test rig. The rig (see Fig. 3) consisted of a rotatable arm holding the motor, torque cell, and propeller in the center of the tunnel. The rotatable arm extended above the tunnel to a lever arm that translated the force from the propeller to a load cell outside the tunnel. A symmetrical fairing was used

Figure 2. Sketch of UIUC 3 ft by 4 ft wind tunnel.[8]

to reduce the drag on the support rigging. Drag on the rigging would decrease the measured thrust and limit the accuracy of the experiment. More details covering the experimental setup can be found in Uhlig.[10]
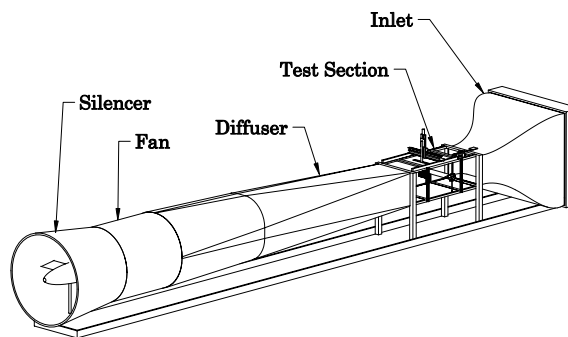
Data was recorded using a National Instruments analog-to-digital board connected to a personal computer. The voltage values were translated to units using calibration curves. The load cell that measured propeller thrust and the torque cell that measured motor torque were calibrated regularly (at least every 48 hours). The thermocouple and ambient pressure were compared to additional sources for temperature and pressure measurements. The measurements were consistent and repeatable.

To calibrate the load cell, a pulley allowed precisely measured weights to exert a load on the test stand at the same location as the propeller hub. The weights were gradually increased and then decreased to develop

American Institute of Aeronautics and Astronautics

a detailed understanding of the relationship between voltages and thrust amounts. From the resulting linear relationship, a calibration curve was determined.

The propeller speed (RPM) was sampled at 20,000 Hz due to its high speed. The thrust, torque, temperature and pressure (ambient and dynamic) were sampled at a lower 3,000 Hz. The propeller speed was sampled first followed immediately by the second slower sampling of the other items.

To begin a test, a number of items were set in the software to correspond to the specific propeller. In each case the initial run was a static run in the wind tunnel with the sides of the tunnel open to allow static freestream flow conditions. Once the RPM range, number of data points, and number of data acquisitions at each point were set, the software would automatically run through the tests and acquired the data.

For runs over a range of advance ratios sweeping over a range of freestream speeds, additional settings were needed. A range of wind tunnel velocities were set with a 2 ft/sec increment. To measure the freestream dynamic pressure a 1-torr transducer was used for speeds of 8 ft/sec to 40 ft/sec and a 10-torr transducer was used for 34 ft/sec to 80 ft/sec. Initially, the 1-torr run was completed; then if required a second high speed run was completed with the 10-torr transducer. Each test over a range of advance ratios was at one propeller RPM setting. The upper limit of the speed of the wind tunnel was set by the lower of two parameters. First, testing was stopped if the propeller net thrust approached zero. At this

Figure 3. Test stand viewed from above.[6, 7]

point the freestream drag on the propeller was more than the thrust on the propeller resulting in an unloading of the tension on the load cell. The load cell was designed to operate in tension only, not compression, so the testing was stopped to preserve the load cell. The second reason testing was stopped was the lack of propeller net torque. This occurs at high freestream speed when the propeller starts to work as a windmill. To prevent this, testing was stopped as the torque approached zero.
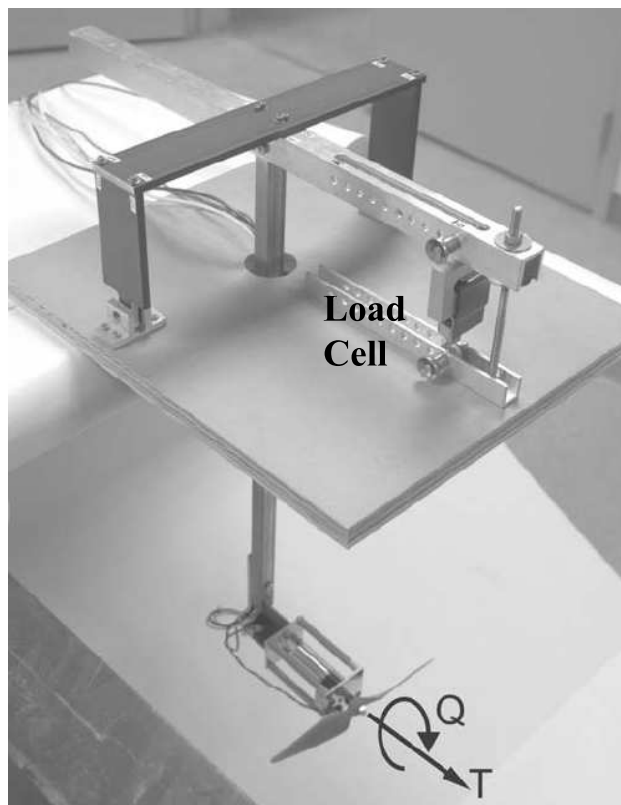
III.   Experimental Data

A set of variable pitch propellers manufactured by Ramoser Technik + Design under the varioPROP name was selected because of the settable pitch and the variety of shapes available. The 'D' propellers had diameters of 6.0, 7.0, 7.9, 8.1, 8.9, and 9.9 in. Two 'G' propellers, 8.0 and 7.1 in. diameters, were selected along with one 9.7 in. 'SG' propeller. Each propeller was tested at three pitch settings. The settings corresponded to a low, medium, and high pitch setting.

American Institute of Aeronautics and Astronautics

The experimental data confirmed some expected results. Increasing pitch increased the advance ratio of peak efficiency, and the greatest efficiency occurred at the medium pitch setting. Performance increased with propeller speed as previously noted by Brandt[6] and Tehrani.[7] The increase was due to better airfoil performance as Reynolds numbers increased. Changes in the propeller speed had the largest effect when the propeller was operating over a wide range of Reynolds numbers and the propeller airfoil sections were operating at high lift-to-drag ratios. When operating at high or low angles of attack airfoil performance becomes less dependent on Reynolds number. An airfoil often has significant nonlinearities in the lift curve slope as the Reynolds number decreases below its designed range. Changes in the lift curve slope would cause the propeller efficiency to decrease as the propeller speed is decreased and the Reynolds number decreased.

In Figs. 5–6, the results for two Ramoser Technik + Design varioPROP propeller are shown. Each propeller was tested at three pitch settings. The nominal pitch measurement given in the legend is the angle measured at 75% radius. The propeller data versus advance ratio (η, C_T, and C_P vs. J) were plotted for multiple propeller RPM settings.
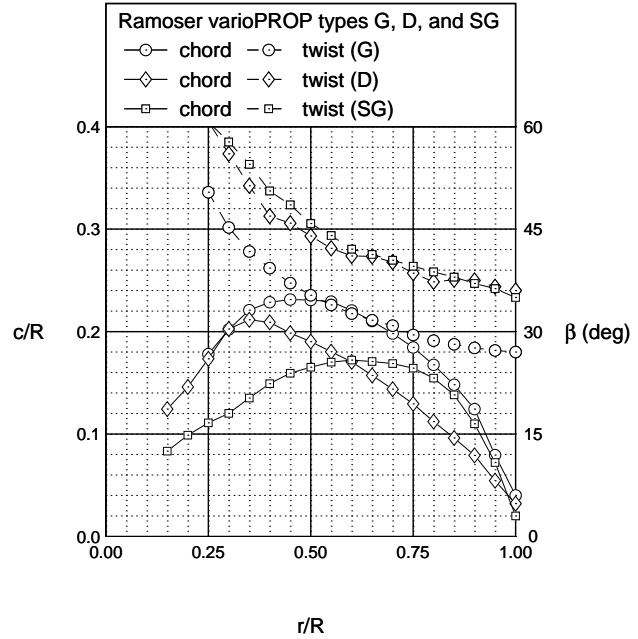

Figure 4. The three types of geometry for the Ramoser Technik + Design propellers measured at high pitch.

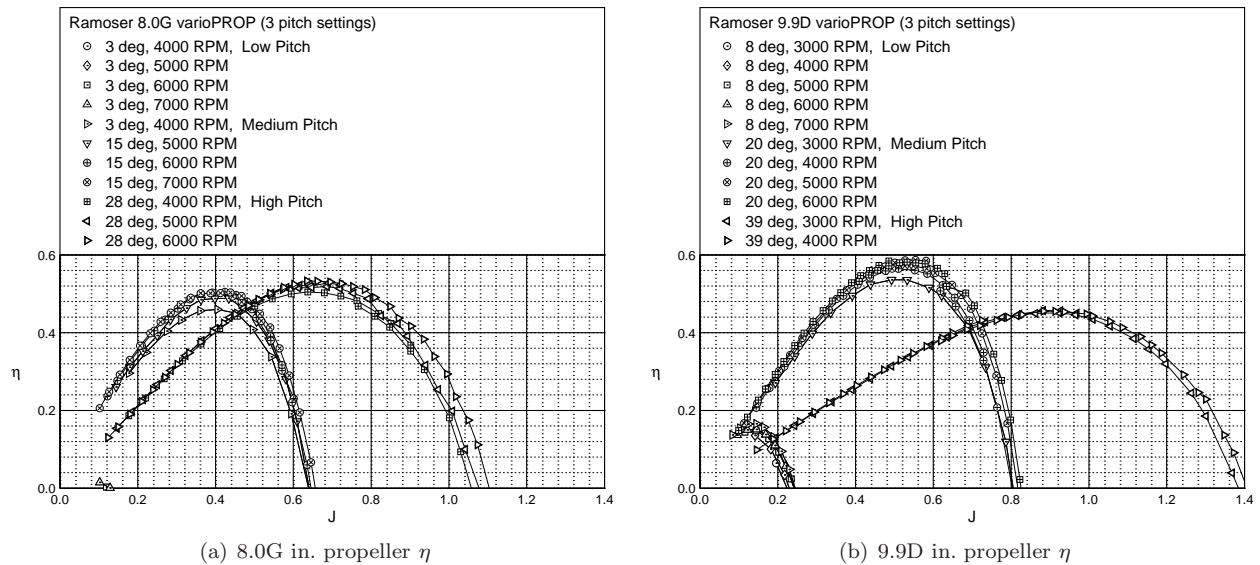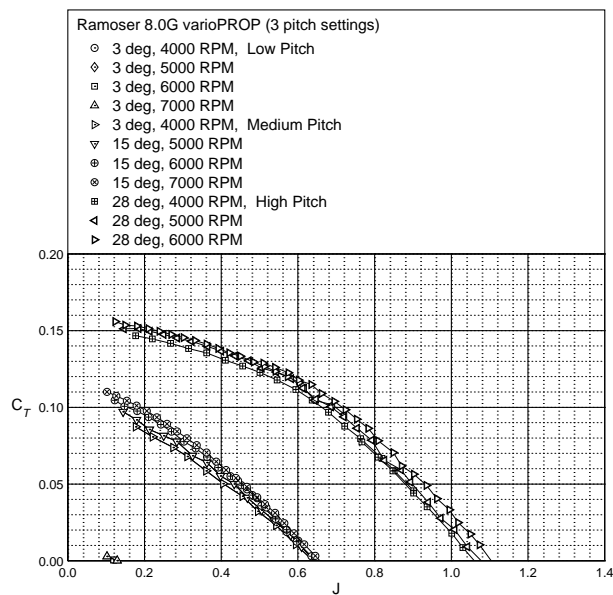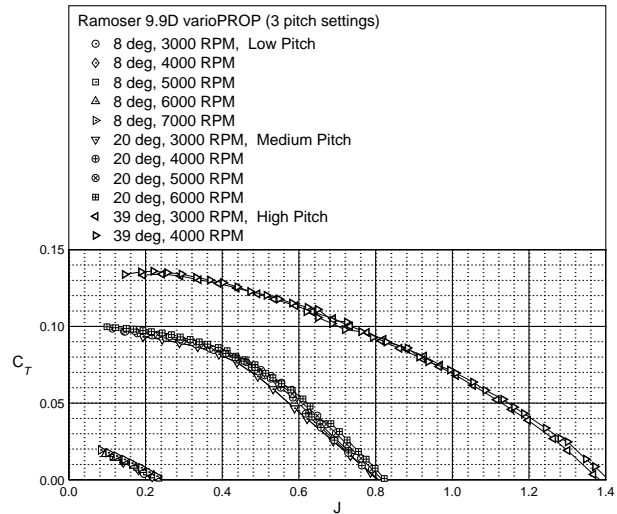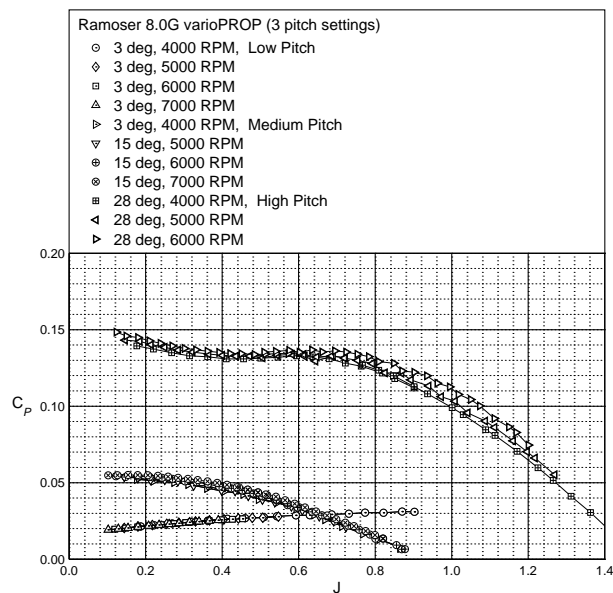(a) 8.0G in. propeller η

(b) 9.9D in. propeller η

Figure 5. Propeller efficiency for two propellers at three pitch settings over a range of RPM settings.

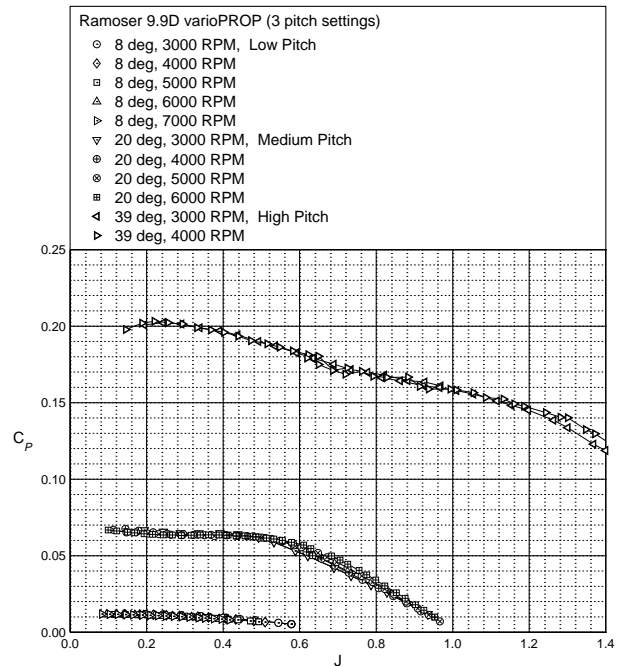American Institute of Aeronautics and Astronautics

(a) 8.0G in. propeller C_T

(b) 9.9D in. propeller C_T

(c) 8.0G in. propeller C_P

(d) 9.9D in. propeller C_P

Figure 6. Propeller thrust and power coefficient for two propellers at three pitch settings over a range of RPM settings.

American Institute of Aeronautics and Astronautics

IV.   Calculation of Predicted Results

Blade Element Momentum Theory (BEMT) was used to generate calculated results. PROPID is a computer code developed to analyze and design horizontal axis wind turbines. It is based upon existing propeller codes, including PROP, that uses a BEMT approach to calculate performance.[1,4] Although PROPID has been mainly developed to desgin and analyze wind turbines, the code had the ability to design and analyze propellers. To analyze the current propellers, the input file required propeller geometry and airfoil performance data. The results from PROPID were compared with the measured experimental propeller performance data to better understand the post-stall behavior of the Ramoser Technik + Design varioPROP propellers.

Figure 7. A scan of the blade cross section with the points resulting from the spline.

To accurately predict performance using BEMT, an accurate twist distribution, chord distribution and airfoil cross section data were needed. To acquire these data, two techniques were used. First, digital images were used in PropellerScanner to generate twist and chord distributions on all propellers.[11] Second, selected propellers were digitized by measuring sections (slices) to achieve more accurate results.

To measure the sections, each blade was placed in solidifying gel normally used for 'water' in artificial flower arrangements. These substances were selected because they did not heat during the curing process and the finished product was a hard sliceable block. The brands used were a Garden Splendor® Quick Water™ kit, a Le Silk Shoppe® Acrylic Water kit and an Everlasting Elegance® kit. Everlasting Elegance® was the best since it cured to a harder state than the others and did so relatively quickly.

A typical slice of the propeller was taken every 0.20 to 0.25 in. resulting in ten cross sections for an 8 in. propeller. A typical cross section is shown in Fig. 7. At each slice, the twist, chord, and distance from the hub were recorded. Additionally the airfoil

Figure 8. Ramoser Technik + Design varioPROP 8.1 'D' propeller geometry from two difference slices and PropellerScanner

coordinates were found by importing the scanned images into a CAD program. A spline was then placed around the edge of the shape resulting in a set of smooth coordinates tracing the edge of the airfoil.

A number of Ramoser Technik + Design varioPROP propellers were digitized in this way by measuring sections. The 8.1 in. propeller was sliced twice to compare results and reliability of this method. The results for two slices demonstrated that the technique was repeatable as seen in Fig. 8. It is worth noting that the 8.1 in. 'D' differs somewhat from the rest of the 'D' family of blades.

At four radial locations (approximately 30%, 50%, 75% and 90–100%) the cross sections were scanned and a line splice was placed along the edge. The coordinates of the line were used to define the measured airfoil and were used to calculate airfoil performance. The lift and drag were a function of angle of attack and Reynolds number. The two main areas of data required were angles of attack beyond stall and moderate angles of attack before stall. Data from different sources were combined to form the total result.

For moderate angles of attack, XFOIL[12] was used to calculate the airfoil performance at a set of Reynolds numbers. While experimental data would have been ideal, it was not available. The predicted $C_{l,max}$ from XFOIL was decreased by 10% based on experience with XFOIL. XFOIL data was used from the negative stall to the positive stall. Beyond stall, the lift and drag were based on flat plate theory. This approach was supported by other research.[2,13] The 2-D airfoil data is shown in Fig. 9.a.

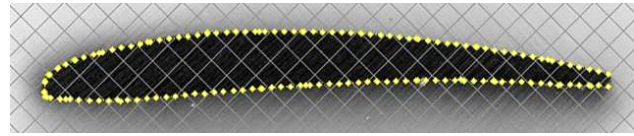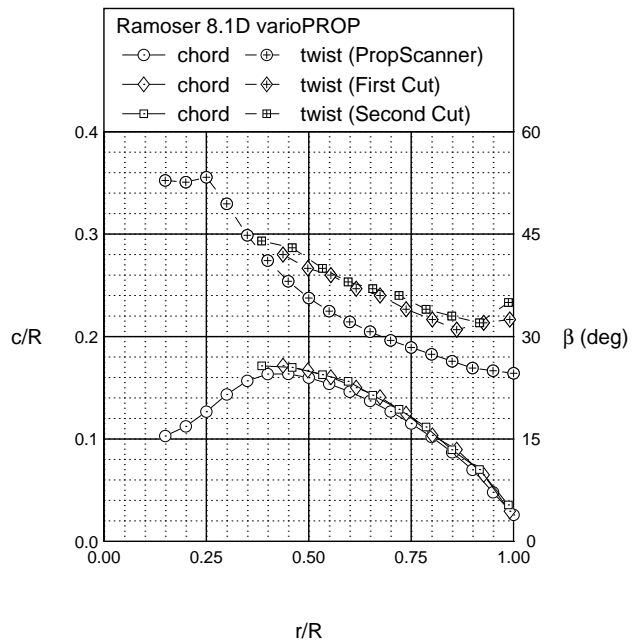A number of stall delay models were included in PROPID, including the Corrigan model. It shifted the
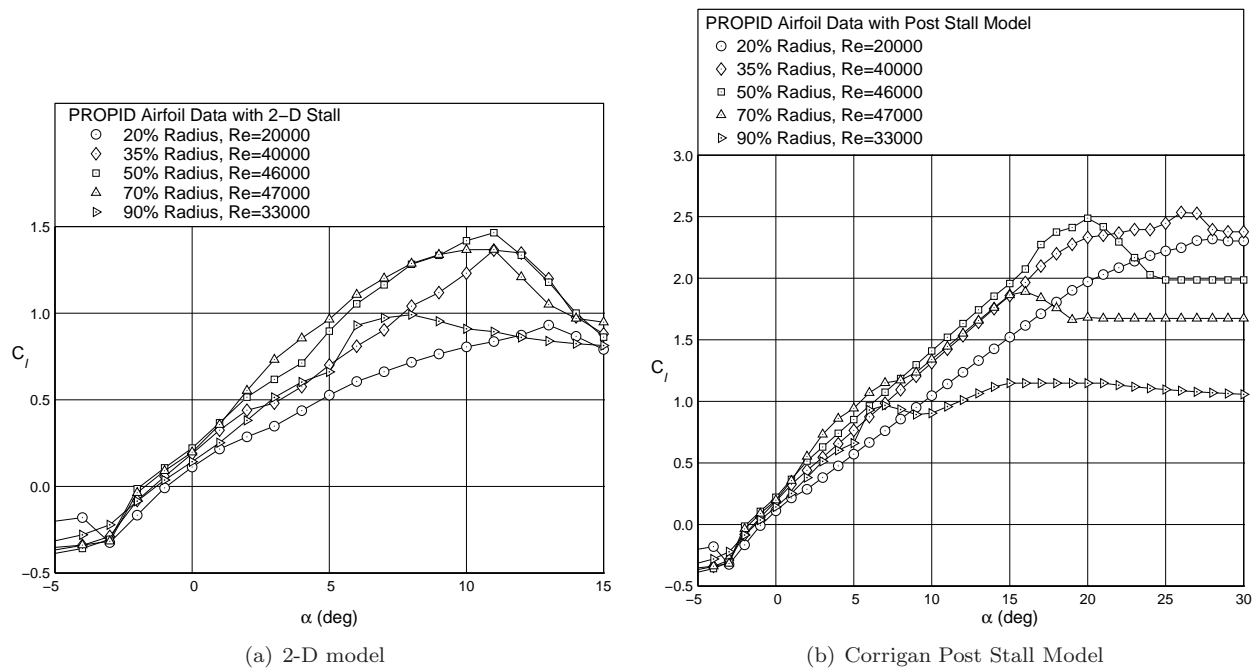
American Institute of Aeronautics and Astronautics

Figure 9. Airfoil performance with and without post stall models.

$C_{l,max}$ to a higher values at a higher angle and placed a standard 2π lift curve slope in the gap[4] as seen in Fig. 9.b. Pre-stall C_d shifted to angles greater then stall and the data was expanded to fit the greater range of angles. The model (consistent with 3-D post-stall aerodynamic phenomenon) results in $C_{l,max}$ being much higher than the 2-D predictions near the blade root. The outboard sections had minimal post-stall corrections, while the three inboard airfoils had a significant shift to higher C_l.

V.   Comparison to Predicted Results

To understand where post-stall behavior was occurring, the experimental results were compared with predicted results. PROPID was used to calculate results for the different geometries. By comparing the predicted results with the experimental results, a better understanding of propeller post-stall aerodynamics can be developed.

Figure. 10 shows the experimental data and predictions for the 9.9D propeller. The predictions include those with and without a stall delay correction that models the 3D post-stall aerodynamics. For the low and medium pitch settings where post-stall effects are negligible, the predictions showing C_T and C_P are in relatively good agreement with experiment.

For the high pitch setting, there are significant discrepancies. The differences increase with decreasing advance ratio, which corresponds to increasing angle of attack. Overall the worse predictions are those corresponding to the case without the stall delay model where the C_T is under predicted. Since the thrust is driven largely by the lift coefficient, it is clear that in the experiment higher $C_{l,max}$ is being realized by 3-D post-stall effects. The predictions are improved by using a stall delay model which increases $C_{l,max}$ (see Fig. 9.b), in this case the Corrigan stall delay model within PROPID. It should be noted that some of the discrepancies are due to uncertainty in the pitch measurement and airfoil performance. With regard to the latter, the Corrigan model and other 3-D post-stall models are empirical and require tuning before they can be used reliably outside of validation cases.
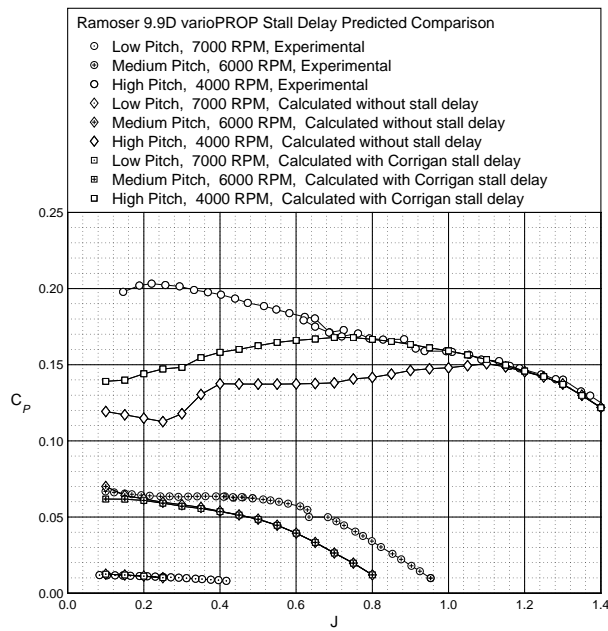
VI.   Conclusion

Rotational 3-D post-stall effects have been documented on wind turbines[2] and full-scale propellers,[5] and now as this paper shows these same effects are observed on small-scale low Reynolds number propellers. Codes

American Institute of Aeronautics and Astronautics
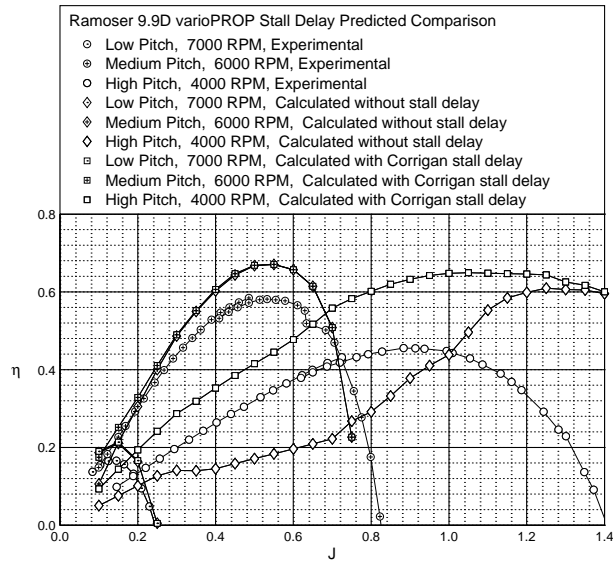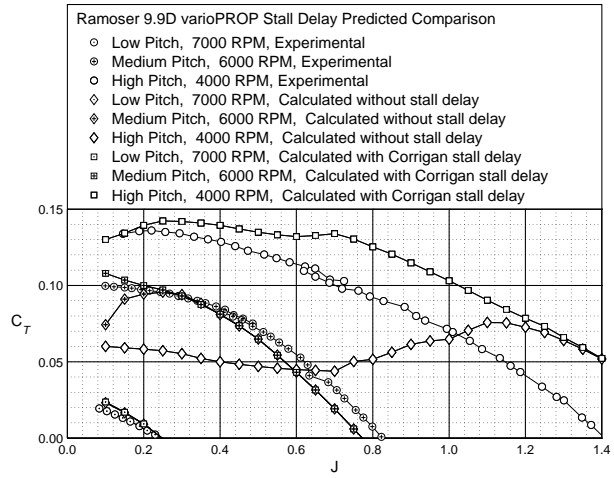
(a) 9.9D in. propeller η

(b) 9.9D in. propeller C_T

(c) 9.9D in. propeller C_P

Figure 10. Predicted (with and without a stall delay model) and experimental efficient and the coefficient of thrust and power for 9.9D propeller at three pitch settings.

like PROPID that rely on blade-element momentum theory adequately predict performance in the normal working range of operation, but in the post-stall regime significant 3-D effects lead to large discrepancies between experiment and predictions that use only 2-D airfoil data. Using a stall delay model that takes into account the increase in lift owing to rotational 3-D post-stall effects can begin to simulate the effects of the underlying physics. However, such stall delay models are empirical and hence rely on experimental data for their refinement and ultimate applicability. The research documented here and included in-depth in Uhlig[10] begins to pave the way for future improvements in rotational 3-D post-stall modeling for propellers and wind turbines.

References

[1]Selig, M. S. and Tangler, J. L., "Development and Application of a Multipoint Inverse Design Method for Horizontal Axis Wind Turbines," *Wind Engineering*, Vol. 19, No. 2, 1995.

[2]Tangler, J. L. and Kocurek, J. D., "Wind Turbine Post-Stall Airfoil Performance Characteristics Guidelines for Blade-Element Momentum Methods," *AIAA Aerospace Sciences*, Vol. 42, No. 2, 2004, pp. 1–10.

[3]Himmelskamp, H., *Profile Invesgitation on Rotating Airscrews*, Ph.D. thesis, Göttinggen, Germany, 1945.

[4]Selig, M. S., *PROPID User Manual (Beta Version 3.0)*, University of Illinois at Urbana–Champaign, 1998.

[5]Gur, O. and Rosen, A., "Propeller Performance at Low Advance Ratio," *AIAA Journal of Aircraft*, Vol. 42, No. 2, 2005, pp. 435–441.

[6]Brandt, J., *Small-Scale Propeller Performance at Low Speeds*, Master's Thesis, University of Illinois at Urbana-Champaign, Department of Aeronautical and Astronautical Engineering, 2005.

[7]Tehrani, K., *Propellers in Yaw at Low Speeds*, Master's Thesis, University of Illinois at Urbana-Champaign, Department of Aerospace Engineering, 2006.

[8]Selig, M. S. and McGranahan, B. D., "Wind Tunnel Aerodynamic Tests of Six Airfoils for Use on Small Wind Turbines," Tech. rep., National Renewable Energy Laboratory, NREL/SR-500-34515, 2004.

[9]Selig, M. S., Guglielmo, J. J., Broeren, A. P., and Giguère, P., *Summary of Low-Speed Airfoil Data, Vol. 1*, SoarTech Publications, Virginia Beach, Virginia, 1995.

[10]Uhlig, D. V., *Post Stall Propeller Behavoir at Low Reynolds Numbers*, Master's Thesis, University of Illinois at Urbana-Champaign, Department of Aerospace Engineering, 2007.

[11]Hepperle, M., *PropellerScanner Manual*, MH AeroTools, www.mh-aerotools.de, 2003.

[12]Drela, M. and Youngren, H., *XFOIL 6.9 User Primer*, Massachusetts Institute of Technology, 2001.

[13]Sheldahl, R. and Klimas, P., "Aerodynamic Characteristics of Seven Symmetrical Airfoil Sections Through 180-Degree Angle of Attack for Use in Aerodynamic Analysis of Vertical Axis Wind Turbines," Tech. rep., Sandia National Laboratories, SAND80-2114, 1981.